SOP TRANSACTIONS ON THEORETICAL PHYSICS
ISSN(Print): 2372-2487 ISSN(Online): 2372-2495
DOI: 10.15764/TPHY.2014.03003
Volume 1, Number 3, September 2014

SOP TRANSACTIONS ON THEORETICAL PHYSICS

Kullback-Leibler Approach to Chaotic Time Series

Andres Kowalski[1,2*], Maria Teresa Martin[1,3], Angelo Plastino[1,3,5], George Judge[4]

[1] *Instituto de Física (IFLP-CCT-Conicet), Fac. de Ciencias Exactas, Universidad Nacional de La Plata, C.C. 727, 1900 La Plata, Argentina.*

[2] *Comision de Investigaciones Científicas (CIC).*

[3] *Argentina's National Research Council (CONICET).*

[4] *207 Giannini Hall, University of California, Berkeley, Berkeley, CA 94720, USA.*

[5] *hysics Department and IFISC-CSIC, University of Balearic Islands, 07122, Palma de Mallorca, Spain*

***Corresponding author**: kowalski@fisica.unlp.edu.ar

Abstract:
We focus discussion on extracting probability distribution functions (PDFs) from semi-chaotic time series (TS). We wish to ascertain what is the best extraction approach and to such an end we use an extremely well known semiclassical system in its classical limit [1, 2]. Since this systems possesses a very rich dynamics, it can safely be regarded as representative of many other physical scenarios. In discussing this "extraction" problem, we consider the two most natural approaches, namely, i) histograms and ii) the Bandt–Pompe technique. We use the Kullback-Leibler relative entropy to compare the information content of the concomitant PDFs.

Keywords:
Kullback-Leibler-distance; Semiquantum Physics; Chaos

1. INTRODUCTION

Information extracted from time series (TS) data, originating from diverse natural processes, may be conveyed by probabilistic distribution functions (PDFs) [3]. What is the appropriate technique to best build up these PDFs from a given time series? The data at our disposal always possess a stochastic component due to noise [4, 5], so that different procedures attain diverse quality degrees.

The extraction procedures constitute our main concern here. We wish to ascertain what is the best extraction approach and to such an end we use an extremely well known semiclassical system in its trajectory towards classical limit [1, 2]. Since this systems possesses a very rich dynamics, it can safely be regarded as representative of many other physical scenarios [1, 2]. The system's dynamics exhibits regulars zones, chaotic ones and other regions that, although not chaotic, display complex features. Form a purely dynamic viewpoint the systems has been exhaustively investigated [2]. This is also the case in which the research has been made via statistical techniques, like Entropy and Statistical Complexity [6]. Consequently, one can safely concentrate efforts on the appropriateness of different extraction techniques, that pose the only questions to be answered here. We will focus attention on two popular PDF methodologies and discuss their information-content. We will deal with the histogram

approach [7] and with Bandt and Pompe's Methodology (BP) [8]. Even if one might guess that the BP methodology would be the best one, it is still important to carefully assess just in which of the regions (or for what dynamical features) its performance is more satisfactory.

Our mail tools will be the Kullback-Leibler relative entropy [9] and the Cressie-Read divergence [10]. Note that relative entropies can be regarded as pseudo-distances in probability space. Here we use them to establish just what is the amount of information that one methodology gains with respect to another one.

The two extraction procedures mentioned above are discussed in Section II. Section III briefly recapitulates notions concerning the Kullback-Leibler relative entropy and the CR-divergence family of entropic functionals [10]. A test-scenario is described in Section IV and the concomitant results presented in Section V. Finally, some conclusions are drawn in Section VI.

2. TWO USUAL EXTRACTION TECHNIQUES

In this Section we generate an appropriate time-series (TS) and proceed to extract from it a suitable PDF. The crucial issue is getting a PDF that will properly "capture" either the physics at hand, the nature of the associated underlying natural process, and/or the features of the TS-generating nonlinear dynamical system. Two methodologies have became rather popular in this respect, PDF based on histograms [7] and PDF based on Bandt and Pompe's Methodology [8]. We describe them below.

2.1 PDF Based on Histograms

In order to extract a PDF via amplitude-statistics, the interval $[a,b]$ (with respectively a and b the minimum and maximum of the time series $\mathscr{S}(t) = \{x_t; t = 1, \cdots, M\}$) is first divided into a finite number N_{bin} of non-overlapping subintervals A_i: $[a,b] = \bigcup_{i=1}^{N_{bin}} A_i$ and $A_i \bigcap A_j = \emptyset$, $\forall i \neq j$. One may then employ the usual histogram-method, which is based on counting the relative frequencies of the time series values within each subinterval.

The resulting PDF lacks any information regarding temporal ordering (temporal causality). The only pieces of information that result are the x_t-values that allow one to assign inclusion within a given bin, and this ignores the temporal order (the subindex t). In addition, it is necessary to consider a judiciously chosen optimal value for N_{bin} (see De Micco *et al.* [7]).

2.2 PDF Based on Bandt and Pompe's Methodology

To use the Bandt and Pompe [8] methodology for evaluating the probability distribution P associated with the time series (dynamical system), one starts by considering partitions of the pertinent D-dimensional space that will hopefully "reveal" relevant details of the ordinal structure of a given one-dimensional time series $\mathscr{S}(t) = \{x_t; t = 1, \cdots, M\}$, with embedding dimension $D > 1$ and time delay τ.

We will take here $\tau = 1$ as the time delay [8] and be interested in "ordinal patterns", of order D [8, 11], generated by

$$(s) \mapsto \left(x_{s-(D-1)}, x_{s-(D-2)}, \cdots, x_{s-1}, x_s \right), \tag{1}$$

which assigns to each time s the D-dimensional vector of values at times $s, s-1, \cdots, s-(D-1)$. Clearly, the greater the $D-$value, the more information on the past is incorporated into our vectors. By

"ordinal pattern" related to the time (s), we mean the permutation $\pi = (r_0, r_1, \cdots, r_{D-1})$ of $[0, 1, \cdots, D-1]$ defined by

$$x_{s-r_{D-1}} \leq x_{s-r_{D-2}} \leq \cdots \leq x_{s-r_1} \leq x_{s-r_0}. \tag{2}$$

In this way the vector defined by (1) is converted into a unique symbol $\hat{x}_i$. Thus, a permutation probability distribution $P_x = \{p(\hat{x}_i), i = 1, \ldots, D!\}$ is obtained from the time series x_i. The probability distribution P is obtained once we fix the embedding dimension D and the time delay τ. The former parameter plays an important role for the evaluation of the appropriate probability distribution, since D determines the number of accessible states, $D!$, and tells us about the necessary length M of the time series needed in order to work with a reliable statistics, *i.e.* it must be $D! \ll M$. In particular, Bandt and Pompe [8] suggest for practical purposes to work with $3 \leq D \leq 7$. For more details see [11].

3. KULLBACK-LEIBLER RELATIVE ENTROPY AND CRESSIE-READ FAMILY OF DIVERGENCES

Our goal is to assess the informational content of the two methodologies reviewed above. To this end we use Kullback-Leibler's (KL) divergence or relative entropy [9]. This measure provides an objective assessment of how much information a given PDF contains relative to a second PDF. KL measures the expected number of extra bits required to code samples from p when using a code based on q, rather than using a code based on p [9].

For two normalized, discrete probability distribution functions (PDF) p and q, one has

$$D_{\mathrm{KL}}(p,q) = \sum_{i=1}^{n} \ln\left(\frac{p_i}{q_i}\right) p_i \tag{3}$$

with $D_{\mathrm{KLsn}}(p,q) \geq 0$. $D_{\mathrm{KL}}(p,q) = 0$ if and only if $p = q$ [9]. Being probabilities, usual PDF features like p_i, $q_i \in [0,1]$ for all values of i are assumed. Also, $q_i \neq 0$, for all values of i. The q_i's are interpreted as reference probabilities. It is convenient to work with a normalized KL-version, for the sake of a better comparison between different results. If we divide by $\ln n$ $(n \neq 1)$ corresponding to KL for the certainty vs. the equiprobability case, so that expression (3) becomes

$$D^N_{\mathrm{KL}}(p,q) = \frac{1}{\ln n} \sum_{i=1}^{n} \ln\left(\frac{p_i}{q_i}\right) p_i \tag{4}$$

with $0 \leq D^N_{\mathrm{KL}} \leq 1$. We will work with (4).

Given two PDFs p and q, $D^N_{\mathrm{KL}}(p,q)$ permits us to determine what new information is contained in p relative to that contained in q. If q is a uniform PDF, it conveys no information and KL measures the information content of p. In the present analysis p will be associated with the Bandt–Pompe PDF and q with the histogram procedure (occasionally we also use a p associated to the histogram procedure and a q that represents the uniform PDF).

KL can be seen as a particular case of the Cressie-Read (CR) family of goodness of fit-power divergence measures [10]

$$I(p,q,\gamma) = \frac{1}{\gamma(\gamma+1)} \sum_{i=1}^{n} p_i \left[\left(\frac{p_i}{q_i}\right)^{\gamma} - 1\right] \tag{5}$$

where γ is a parameter that indexes members of the CR family. In the two special cases where $\gamma = 0$ or -1, the notation $I(p,q,0)$ and $I(p,q,-1)$ are to be interpreted as the continuous limits, $\lim_{\gamma \to 0}$

or $\lim_{\gamma\to -1}$, respectively [10]. The $\gamma = 0$ case, corresponds to $D_{\rm KL}(p,q)$ [10]. On the other hand, $I(p,q,-1) = D_{\rm KL}(q,p)$ [10]. We assume that $q_i \neq 0$, for all values of i. It is also convenient to employ a normalized $I(p,q,\gamma)-$version for comparison purposes. So as to normalize the expression (5), we consider $\gamma \geq 0$ in our studies and divide by $(n^\gamma - 1)/\gamma(\gamma+1)$ $(n \neq 1)$ in the case of computing $I(p,q,\gamma)$ for the certainty vs. the equiprobability case. One has

$$I^N(p,q,\gamma) = \frac{1}{n^\gamma - 1} \sum_{i=1}^{n} p_i [(\frac{p_i}{q_i})^\gamma - 1] \tag{6}$$

One finds $0 \leq I^N(p,q,\gamma) \leq 1$. $I^N(p,q,\gamma) = 0$, if and only if $p = q$. One sees that the normalized Kullback-Leibler divergence given by (4) is equal the normalized CR given by (6), with $\gamma \to 0$. Note that $I(p,q,\gamma)$ tends to the Kullback-Leibler divergence $D_{\rm KL}(p,q)$ (see above) and that $(n^\gamma - 1)/\gamma(\gamma+1)$ tends to $\ln n$ when $\gamma \to 0$.

The CR family of power divergences is defined through a class of additive convex functions [10] and the CR power divergence measure encompasses a broad family of test statistics that leads to a broad family of likelihood functions within a moments-based estimation context. In an extremum metrics scenario [10] the general Cressie-Read family of power divergence statistics represents a flexible family of pseudo-distance measures from which to derive empirical probabilities associated with indirect noisy micro and macro data [10].

As γ varies, the resulting estimators that minimize power divergence exhibit qualitatively different sampling behaviors. In the preliminary work of [3] we used $\gamma = 1$.

4. APPLICATION: CLASSICAL-QUANTUM TRANSITION

We test our PDF-extracting approaches with reference to an important physical problem. The classical limit of quantum mechanics (CLQM) is a subject that continues to attract much attention, and can be regarded as one of the frontiers of physics research [12–16]. Certainly, it is the source of much exciting discussion (see, for instance, [12, 13] and references therein). Of particular interest is the issue of "quantum" chaotic motion with regards to the so-called classical limit. Recent efforts by different authors can be consulted in [17] and references therein. It is also of interest the generalized uncertainty principle (GUP) approach ([18, 19]).

Since the introduction of the decoherence concept (1980s) by Zeh, Zurek, Habib [14–16] and others, the emergence of the classical world from Quantum Mechanics has become a subject of great interest. Much insight may be derived from semiclassical perspectives. Several approaches exist: the historical WKB and Born–Oppenheimer approaches, *etc.* The two-interacting systems, considered by Bonilla and Guinea [20], Cooper *et al.* [1], and Kowalski *et al.* [2, 21], constitute composite models in which one system is classical and the other is quantal. This makes sense whenever the quantum effects of one of the two systems are negligible in comparison to those of the other one [2]. Examples include Bloch equations, two-level systems interacting with an electromagnetic field within a cavity and collective nuclear motion. We deal with a special bipartite system that represents the zero-th mode contribution of a strong external field to the production of charged meson pairs [1, 2]. The corresponding Hamiltonian is

$$\hat{H} = \frac{1}{2}\left(\frac{\hat{p}^2}{m_q} + \frac{{P_A}^2}{m_{cl}} + m_q \omega^2 \hat{x}^2 \right) \tag{7}$$

where, *(i)* $\hat{x}$ and $\hat{p}$ are quantum operators, *(ii)* A and P_A are classical canonical conjugate variables and *(iii)* $\omega^2 = {\omega_q}^2 + e^2A^2$ is an interaction term that introduces nonlinearity, where ω_q is a frequency. The quantities m_q and m_{cl} are masses, corresponding to the quantum and classical systems, respectively. As

shown in [21], in dealing with (7), one faces the following autonomous system of nonlinear coupled equations

$$\frac{d\langle\hat{x}^2\rangle}{dt} = \frac{\langle\hat{L}\rangle}{m_q}; \quad \frac{d\langle\hat{p}^2\rangle}{dt} = -m_q\,\omega^2\langle\hat{L}\rangle;$$

$$\frac{d\langle\hat{L}\rangle}{dt} = 2(\frac{\langle\hat{p}^2\rangle}{m_q} - m_q\,\omega^2\langle\hat{x}^2\rangle);$$

$$\frac{d\langle\hat{L}\rangle}{dt} = 2(\frac{\langle\hat{p}^2\rangle}{m_q} - m_q\,\omega^2\langle\hat{x}^2\rangle); \quad \frac{dA}{dt} = \frac{P_A}{m_{cl}}; \frac{dP_A}{dt} = -e^2 m_q A\langle\hat{x}^2\rangle;$$

$$\hat{L} = \hat{x}\hat{p} + \hat{p}\hat{x} \tag{8}$$

The system given by (8) is derived from Ehrenfest's relations

for quantum variables and canonical Hamilton's equations for classical ones [21]. To study the classical limit we also need to consider the classical counterpart of the Hamiltonian given by (7), where all the variables are classical. Recourse to Hamilton's equations allows one to find the classical version of (8); see Ref. [21] for further details. These equations are identical in form to (8) after suitable replacement of quantum mean values by classical variables. The classical limit is obtained by letting the "relative energy" [2]

$$E_r \;=\; \frac{|E|}{I^{1/2}\omega_q} \to \infty \tag{9}$$

where E is the total energy of the system and I is an invariant of the motion described by the system of equations previously introduced (8), related to the Uncertainty Principle

$$I \;=\; \langle\hat{x}^2\rangle\langle\hat{p}^2\rangle - \frac{\langle\hat{L}\rangle^2}{4} \geq \frac{\hbar^2}{4} \tag{10}$$

The system requires numerical solution. The analysis of the system is done by plotting quantities of interest against E_r, that ranges in $[1,\infty]$. For $E_r = 1$ the quantum system acquires all the energy $E = I^{1/2}\omega_q$ and the quantal and classical variables gets located at the fixed point $(\langle\hat{x}^2\rangle = I^{1/2}/m_q\omega_q, \langle\hat{p}^2\rangle = I^{1/2}m_q\omega_q, \langle\hat{L}\rangle = 0, A = 0, P_A = 0)$ [21]. Since $A = 0$ the two systems become uncoupled. For $E_r \sim 1$ the system is almost quantal and the dynamics quasi-periodic [2].

As E_r grows, quantum dynamics features are quite quickly lost and one enters a semiclassical region. From a given value ${E_r}^{cl}$, the morphology of the solutions to (8) begins to resemble that of classical curves [2]. Convergence of (8) solutions to the classical ones is achieved. For very large E_r-values, the system is classical. Both types of solutions coincide. We speak of a semiclassical region $1 < E_r < {E_r}^{cl}$. Within such an interval one pinpoints the special value $E_r = {E_r}^{\mathscr{P}}$, where chaos emerges [21]. The relative number of chaotic orbits (with respect to the total number of orbits) grows with E_r and tends to unity for $E_r \to \infty$ [2].

Time series for the system are to be extracted from a "signal" given by the E_r-evolution of appropriate expectation values of the dynamical variables.

5. RESULTS

In obtaining our numerical results we used $m_q = m_{cl} = \omega_q = e = 1$ for the system's parameters. As for the initial conditions needed to investigate things described by (8) we employed $E = 0.6$. Thus, we fixed E and then varied I so as to obtain our different E_r values. We used 41 different values of I. Additionally, we set $\langle L\rangle(0) = L(0) = 0, A(0) = 0$ (both in the quantum and the classical instances), while $x^2(0)$. $\langle x^2\rangle(0)$ adopted values within the intervals $(0, 2E)$, $(E - \sqrt{E^2 - I}, E + \sqrt{E^2 - I})$ with $I \leq E^2$, respectively. Here ${E_r}^{\mathscr{P}} = 3.3282$ and ${E_r}^{cl} = 21.55264$.

We have a signal that represents the system's state at a given E_r. Sampling that signal we extracted several PDFs. One way of doing this is via histograms. Another way is using the B-P approach. In last methodology it is convenient to adopt the largest $D-$value that verifies the condition $D! \ll M$ (see Section 2.2) This value is $D = 6$, because we will deal with vectors with components of at least $M = 5000$ data-points for each orbit. For verification purposes we also used $D = 5$, without detecting appreciable changes. For $D = 6$ we must consider $n = N_{bin} = 720$ in histograms PDF (See (4) and (6)). The condition $q_i \neq 0$, for all values of i (see Section 3) holds for all our PDFs.

Figure 1 illustrates the fact that for $E_r = 1$ (see section 4), $D^N_{\mathrm{KL}}(B-P, histogram)$ vanishes. Only there the dynamics is strictly periodic. For larger E_r-values, it becomes quasi-periodic. The curves become more convoluted as E_r grows and $D^N_{\mathrm{KL}}(B-P, histogram)$ increases quite rapidly, reaching a maximum at $\sim {E_r}^{\mathscr{P}}$. Afterwards, it diminishes and tends eventually to an asymptotic value of $D^N_{\mathrm{KL}}(B-P, histogram) \sim 0.1$ for $E_r \to \infty$. This asymptotic value coincides with the value of $D^N_{\mathrm{KL}}(B-P, histogram)$ calculated with the classic orbits (solutions of the fully classical system), towards which the solutions of the system of (8) converge.

Accordingly, we gather that the BP PDF could contain more information than the associated histogram one for all stages of the process (save for the instance $E_r = 1$). However, we should also consider the quantity $D^N_{\mathrm{KL}}(histogram, B-P)$, expressing the extra informational amount that the histogram PDF might possess vis-a-vis the BP approach. In **Figure 2** we compare the $D^N_{\mathrm{KL}}(B-P, histogram)$, in black, to the $D^N_{\mathrm{KL}}(histogram, B-P)$, in red. We see that, starting at the special "maximal" $E_r \sim {E_r}^{\mathscr{P}}$, as $D^N_{\mathrm{KL}}(B-P, histogram)$ decreases, $D^N_{\mathrm{KL}}(histogram, B-P)$ grows. It eventually tends towards the same value achieved by $D^N_{\mathrm{KL}}(B-P, histogram)$. An useful indicator is $D = D^N_{\mathrm{KL}}(B-P, histogram) - D^N_{\mathrm{KL}}(histogram, B-P)$ [22]. This quantity may be seen as a better measure of the relative information between both PDFs. We can observe in **Figure 2** that D vanishes at both end-point, that is, in the quantum zone and at the classical limit. The associated dynamics are in these zones, respectively, periodic and very chaotic. For the rest of the process one has $D > 0$, and a more complex dynamics (superposition of chaotic curves and non-chaotic, but complex, ones). Accordingly, using D it turns out that it is in this zone that the BP PDF carries more information than the histogram one, specially at the transition zone $1 < E_r < {E_r}^{cl}$. Its appropriateness is more pronounced for complex non-chaotic curves than for the chaotic $E_r > {E_r}^{\mathscr{P}}$ region. As the chaoticity augments, the BP's superiority diminishes, and the two concomitant PDFs have the same asymptotic value. As a check, **Figure 1** displays as well

$$D^N_{\mathrm{KL}}(histogram, uniform) = 1 - \frac{-1}{\ln n}\sum_{i=1}^{n} p_i \ln p_i \tag{11}$$

the normalized *information* of the histogram's PDF, that contains, not surprisingly, more information than the uniform PDF in the chaotic region, as one can appreciate. However, we see that the two involved PDFs are equivalent in the quantal periodic zone and in the quasi-periodic zone (near the quantum zone). We conclude that the histogram PDF detects chaoticity. These results validate preceding findings that employ the Cressie-Read family of measures (with $\gamma = 1$ in (6) reported in [3]). it We note that here

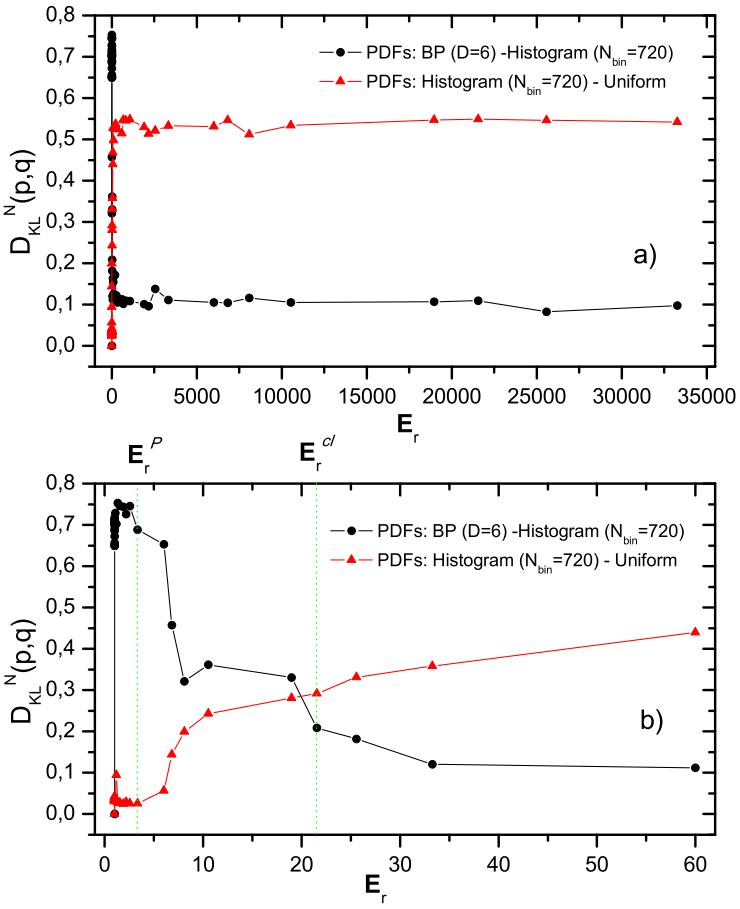

Figure 1. Kullback–Leibler divergence. $D^N_{\mathrm{KL}}(B-P, histogram)$ and $D^N_{\mathrm{KL}}(histogram, uniform)$ are plotted *vs.* E_r. $D^N_{\mathrm{KL}}(B-P, histogram) \geq 0$ in the three stages of the process. In general, it carries more information than the histogram PDF and is much better in the transition zone, $1 < E_r < E_r{}^{cl}$. For $E_r > E_r{}^{\mathscr{P}}$, BP's superiority diminishes. As the chaoticity augments with E_r, the histogram PDF contains more information.

we had at our disposal values very close to $E_r = 1$ that were unavailable in [3] and are here included in **Figure 3** and **Figure 4**.

Comparing now our present results with those of [3] (this entails comparison of **Figure 1**-**Figure 2** with **Figure 3**-**Figure 4**). Note that the maximum within the transition region i) is more pronounced for the CR-divergence and ii) is located at a E_r-value more distant from $E_r{}^{\mathscr{P}}$ than in the KL case. Also, the convergence of $D^N_{\mathrm{KL}}(B-P, histogram)$ and $D^N_{\mathrm{KL}}(histogram, B-P)$ towards the asymptotic values is slower for KL than for CR. This asymptotic value is larger in the $D^N_{\mathrm{KL}}(B-P, histogram)$ case than its CR counterpart. This happens also with reference to $D^N_{\mathrm{KL}}(histogram, uniform)$ asymptotic value.

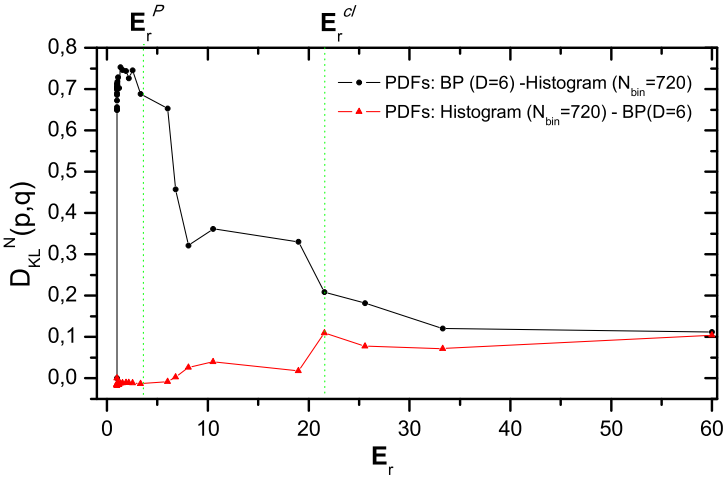

Figure 2. Normalized Kullback–Leibler divergence $D^N_{\mathrm{KL}}(B-P, histogram)$ and $D^N_{\mathrm{KL}}(histogram, B-P)$ are plotted *vs.* E_r. We compare the two quantities. This comparison indicates that the BP approach carries more information than the histogram PDF, save for 1) the quantum zone and 2) the classical limit. As the chaoticity augments, the BP's superiority diminishes, and the two concomitant PDFs have the same asymptotic value.

6. CONCLUSIONS

The study and characterization of time series, by recourse to conventional parametric statistical theory tools, assumes that the underlying probability distribution function (PDF) is given. Several methodologies are available for the purpose. We have focused our attention upon the technique employed so as to extract these PDFs from the concomitant time-series, using as a testing ground a well known semiclassical Hamiltonian in its associated dynamics journey from the quantum region towards the classical limit [1, 2]. Since this systems possesses a very rich dynamics, it can safely be regarded as representative of many other physical scenarios. [1, 2]. The system's dynamics exhibits regulars zones, chaotic ones and other

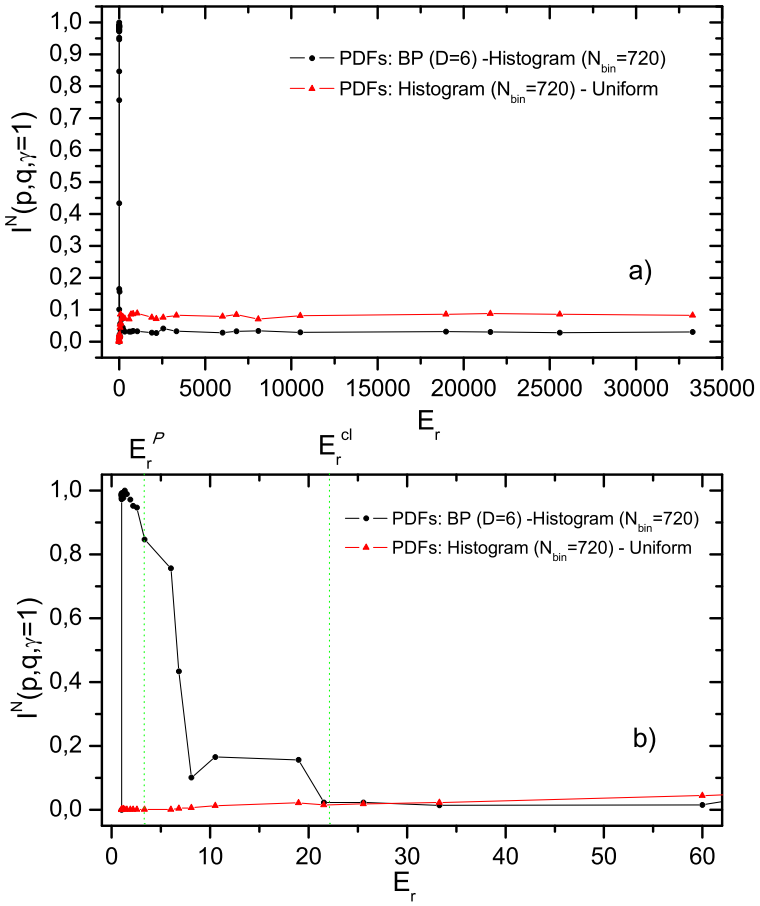

Figure 3. Normalized Cressie-Read divergence ($\gamma = 1$). I(B-P,histogram,1) and I(histogram,uniform,1) are plotted vs. E_r. These graphs show results essentially equivalent to those of **Figure 1**.

regions that, although not chaotic, display complex features.

In discussing this "extraction" problem, we consider the two more natural approaches, namely, i) histograms and [7] ii) the Bandt–Pompe technique [8]. We have employed the Kullback-Leibler relative entropy and the Cressie-Read family of power divergence statistics with $\gamma = 1$ [3], in order to obtain a definite, quantitative assessment of the performance of these methodologies. CR results match KL ones in a close fashion.

We have confirmed the BP-superiority relative to their histogram counterparts. The BP approach carries at least the same information than the histogram one for the three stages of the process. In general, it carries more information que the histogram PDF, save for 1) the quantum zone and 2) the classical limit (**Figure 2** and **Figure 4**) and is much better in the transition zone, where the dynamics is complex but non-chaotic. In the chaotic region, this BP's superiority gradually diminishes (**Figure 1**, **Figure 2**, and

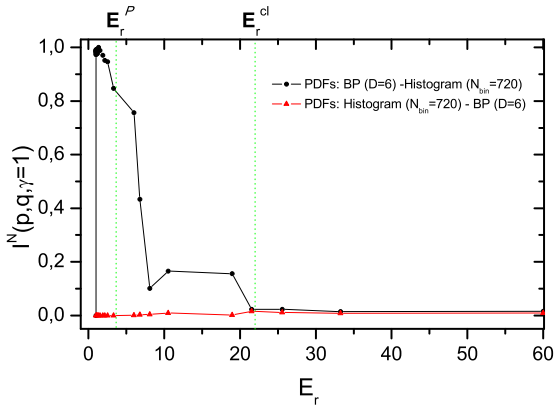

Figure 4. Normalized Cressie–Read divergence ($\gamma = 1$). I(B-P,histogram,1) and I(histogram,B-P,1) are plotted vs. E_r. Again, this graph displays results essentially equivalent to those of **Figure 2**.

Figure 4). Rather surprisingly, at the the classical limit, histogram PDF contains *as much information* as the BP approach and can replace it. We conclude that the histogram PDF detects chaoticity.

Preceding papers have examined the relative merits of the histogram *vs.* the BP approach (for instance, see the excellent review [11] and references therein). However, these approaches utilize **indirect** measures such as Shannon's Entropy or Statistical Complexity (for instance, see [6]). Our work *adds an objective assessment, via the Kullback-Leibler relative entropy and the Cressie-Read divergence*, where PDF-to-PDF direct comparison is feasible.

ACKNOWLEDGMENTS

This work was partially supported by the project PIP1177 of CONICET (Argentina), and the projects FIS2008-00781/FIS (MICINN) - FEDER (EU) (Spain, EU).

References

[1] Cooper, F.; Dawson, J.; Habib, S.; Ryne, R.D. Chaos in time-dependent variational approximations to quantum dynamics. *Phys. Rev. E* **1998**, *57*, 1489–1498.

[2] Kowalski, A.M.; Plastino, A.; Proto, A.N. Classical limits. *Phys. Lett. A* **2002**, *297*, 162–172.

[3] Kowalski, A.M.; Martin, M.T.; Plastino, A; Judge, G. On Extracting Probability Distribution Information from Time Series. *Entropy* **2012**, *14*, 1829–184.

[4] Wold, H. *A Study in the Analysis of Stationary Time Series*; Almqvist and Wiksell: Upsala, Sweden, 1938.

[5] Kurths, J.; Herzel, H. Probability theory and related fields. *Phys. D* **1987** , *25*, 165.

[6] Kowalski, A.M.; Martín, M.T.; Plastino, A.; Rosso, O.A. Bandt-Pompe approach to the classical-quantum transition. *Phys. D* **2007**, *233*, 21–31.

[7] De Micco, L.; González, C.M.; Larrondo, H.A.; Martín, M.T.; Plastino, A.; Rosso, O.A. Randomizing nonlinear maps via symbolic dynamics. *Physica A* **2008**, *87*, 3373–3383.

[8] Bandt, C.; Pompe, B. Permutation entropy: A natural complexity measure for time series. *Phys. Rev. Lett.* **2002**, *88*,174102:1–174102:4.

[9] Kowalski, A.M.; Rossignoli, R.D., Curado, E.M.F. Eds. *Concepts and Recent Advances in Generalized Information Measures and Statistics*; Bentham Science Publishers, 2013.

[10] N. Cressie and T. Read, Journal of the Royal Statistical Society, Series B **46** (1984) 440; *Goodness of Fit Statistics for Discrete Multivariate Data* (Springer, New York, 1988).

[11] Zanin, M.; Zunino, L.; Rosso, O.A.; Papo, D. Permutation entropy and its main biomedical and econophysics applications: A review. *Entropy* **2012**, *14* , 1553–1577.

[12] Halliwell, J.J.; Yearsley, J.M. Arrival times, complex potentials, and decoherent histories. *Phys. Rev. A* **2009**, *79*, 062101:1–062101:17.

[13] Everitt, M.J.; Munro, W.J.; Spiller, T.P. Quantum-classical crossover of a field mode. *Phys. Rev. A* **2009**, *79* , 032328:1–032328:6.

[14] Zeh, H.D. Why Bohms quantum theory? *Found. Phys. Lett.* **1999**, *12*, 197–200.

[15] Zurek, W.H. Pointer basis of quantum apparatus: Into what mixture does the wave packet collapse? *Phys. Rev. D* **1981**, *24*, 1516–1525.

[16] Zurek, W.H. Decoherence, einselection, and the quantum origins of the classical. *Rev. Mod. Phys.* **2003**, *75*, 715–775.

[17] Kowalski, A.M.; Martín, M.T.; Plastino, A.; Proto, A.N. Classical limit and chaotic regime in a semi-quantum hamiltonian. *Int. J. Bifurc. Chaos*, **2003**, *13*, 2315–2325.

[18] Tawfik, A. Impacts of Generalized Uncertainty Principle on Black Hole Thermodynamics and Salecker-Wigner Inequalities. JCAP, , **2003**, *1307*, 040.

[19] El Dahab, E.; Tawfik, A. Measurable Maximal Energy and Minimal Time Interval. e-Print: **2014**, arXiv:1401.3164 [gr-qc].

[20] Bonilla, L.L.; Guinea, F. Collapse of the wave packet and chaos in a model with classical and quantum degrees of freedom. *Phys. Rev. A* **1992**, *45*, 7718–7728.

[21] Kowalski, A.M.; Martín, M.T. ; Nuñez, J.; Plastino, A.; Proto, A.N. Quantitative indicator for semiquantum chaos. *Phys. Rev. A* **1998**, *58*, 2596–2599.

[22] Schreiber, T. Measuring information transfer. *Phys. Rev. Lett.* **2000**, *85*, 461–46.

About This Journal

TPHY is an open access journal published by Scientific Online Publishing. This journal focus on the following scopes (but not limited to):

- Chaos Theory
- Chaotic Cryptography
- Classical and Quantum Gravitation
- Cosmology and Astrophysics
- Fluctuation Phenomena
- Foundational Problems in Theoretical Physics
- Foundations of Quantum Mechanics
- High Energy Physics
- Mathematical Physics
- Modified Gravity Theory
- Nonlinear Phenomena
- Nuclear Physics
- Particle and Nuclear Physics
- Physics of ultra High-energy Cosmic Rays
- Quantum Cryptography
- Quantum Physics
- Relativistic Fluid and Hydrodynamics
- Solid-State Physics
- Time Series Analysis

Welcome to submit your original manuscripts to us. For more information, please visit our website: http://www.scipublish.com/journals/TPHY/

You can click the bellows to follow us:

- Facebook: https://www.facebook.com/scipublish
- Twitter: https://twitter.com/scionlinepub
- LinkedIn: https://www.linkedin.com/company/scientific-online-publishing-usa
- Google+: https://google.com/+ScipublishSOP

SOP welcomes authors to contribute their research outcomes under the following rules:

- Although glad to publish all original and new research achievements, SOP can't bear any misbehavior: plagiarism, forgery or manipulation of experimental data.
- As an international publisher, SOP highly values different cultures and adopts cautious attitude towards religion, politics, race, war and ethics.
- SOP helps to propagate scientific results but shares no responsibility of any legal risks or harmful effects caused by article along with the authors.
- SOP maintains the strictest peer review, but holds a neutral attitude for all the published articles.
- SOP is an open platform, waiting for senior experts serving on the editorial boards to advance the progress of research together.